Structure of Anthrax Adenylyl Cyclase Toxin

W. J. Tang,[1] C. L. Drum,[1,2] S.Yan,[1] J. Bard,[2] Y. Shen,[1] S. Soelaiman,[1] Z. Grabarek,[2] A. Bohm[2]
[1]Ben-May Institute for Cancer Research, The University of Chicago, Chicago, IL, U.S.A.
[2]Boston Biomedical Research Institute, Boston, MA, U.S.A.

Introduction

In October 2002, the United States of America was attacked by mail containing anthrax spores that caused five innocent Americans to die of anthrax infection and led to massive disruption around the globe. The spore of the gram-positive bacterium *Bacillus anthracis* causes anthrax infection. The anthrax bacterium defeats the host defense system by secreting three exotoxins: protective antigen (PA), lethal factor (LF), and edema factor (EF) [1]. PA is a pH-dependent transporter [2]. After binding to a cellular receptor and proteolytic activation by furin, PA assembles into a heptamer [2, 3]. The PA heptamer can then bind both LF and EF. Upon endocytosis and acidification, PA delivers both EF and LF into the cytosol of eukaryotic cells. LF, a zinc metalloprotease, can cleave and inactivate mitogen-activated protein kinase kinase and possibly other cellular proteins in the macrophage [4, 5]. This results in the release of tumor necrosis factor α and interleukin-1 β, which are partly responsible for sudden death in systemic anthrax [1]. EF, a calmodulin (CaM)-activated adenylyl cyclase, can increase the level of intracellular cyclic AMP to a pathologic level, upsetting water homeostasis. EF is believed to be responsible for the massive edema and impaired neutrophil function seen in cutaneous anthrax [1]. Together, LF and EF make anthrax a deadly disease.

EF has two functional domains. The N-terminal 290 amino-acid region of the 92 kDa EF shares sequence similarity to LF and binds PA. The C-terminal 510 amino-acid region of EF exhibits CaM-activated adenylyl cyclase activity and has adenylyl cyclase activity about three orders of magnitude higher than mammalian CaM-activated adenylyl cyclase [6, 7]. Here we report on the structure of the adenylyl cyclase domain of EF with and without its activator, CaM, and address the mechanism of CaM activation and catalysis of EF [8 9].

Methods and Materials

Crystallization

Hexa-histidine tagged edema factor adenylyl cyclase domains, H6-EF3 and EF3-CH6, and human CaM were purified as described [7]. Crystals of EF3/CaM complex and EF alone were grown by the hanging drop method at 4ºC. To grow EF/CaM crystals with space group I222, a protein solution containing 14.6 g/mL EF3-H6 and 6.2 g/mL CaM was mixed with a well solution containing 10% PEG 8,000, 350 mM ammonium sulfate, 100 mM NaCacodylate [pH 6.5], 20% glycerol, 1 mM $MgCl_2$, and 300 μM $YbCl_3$. Lanthanide and 3'-deoxy ATP (5 mM), a nonhydrolyzable ATP analog, both facilitated crystal seeding and growth. To grow crystals of EF alone with space group $P2_12_12$, 1 μL of 40 mg/mL H_6-EF in 20 mM Tris, pH 7.5, 50 mM NaCl, was mixed with 1 μL of a well solution containing 100 mM citric acid (pH 5.65), 15% glycerol, PEG 550MME at 11.5% w/v, 220 mM $NiSO_4$, and 2 mM $MgCl_2$.

Cryoprotection and Data Collection

The approximately 0.4 × 0.4 × 0.6-mm-size crystals of EF/CaM complex were transferred into an identical mother liquor containing 30% glycerol by slowly ramping up glycerol concentration over 24 h. The crystals of EF alone were equilibrated for 5 min in cryoprotectant containing the well buffer with 30% glycerol. Crystals of EF alone and EF/CaM complex were frozen in liquid propane and mounted in a 100K nitrogen stream. For the data of EF3-CH6/seleno-methionyl CaM, an extended x-ray fine structure (EXAFS) experiment was used to find the selenium K edge before data were collected at inflection point, peak, and remote wavelengths. Initially the selenium edge was obscured by background fluorescence from the arsenic moiety of 100-mM cacodylic acid, included as the cryoprotectant buffer. However, narrowing of the band pass of the fluorimeter to selectively amplify the selenium fluorescence allowed accurate tuning of the monochromater to the selenium edge.

Results and Discussion

The structure of EF/CaM complex was initially solved by multiwavelength anomalous diffraction at 3.8-Å resolution by using data collected at the APS Structural Biology Center (SBC) and the signal from the 27 CaM selenomethionines and the three Yb ions in the asymmetric unit. The 3.8-Å experimental phases were extended to 2.75-Å resolution by using the data from the best crystal of EF/CaM/3'dATP and iterative cycles of threefold noncrystallographic symmetry averaging and phase combination. The initial phases for the structures of EF-alone (2.6-Å resolution) were obtained by molecular replacement. The statistics of crystallographic data and refinement are listed in Table 1.

Table 1. Crystallographic and refinement statistics.

Crystallographic data		
Crystal	EF-CH_6-CaM-3'dATP	H_6-EF
Space group	I222	$P2_12_12$
a (Å)	117.60	50.47
b (Å)	167.44	203.60
c (Å)	343.48	74.03
X-ray source	APS, 14-BM-C	APS, 14-BM-C
Resolution (Å)	2.75	2.6
Completeness (%) (last shell)	91.6 (57.2)	98.5 (95.4)
R-sym (last shell)	9.7 (26.4)	8.7 (27.3)
I/σ (last shell)	4.6 (2.8)	5.6 (1.7)
Redundancy (last shell)	10.9 (3.3)	6.5 (4.8)
Refinement data		
Resolution (Å)	20-2.75	30-2.6
R-factor/free (%)	21.5/28.6	22.8/27.6
Bond length (Å)	0.005	0.011
Bond angle (degree)	1.8	1.55

The molecular structure of the catalytic domain of EF is novel and composed of three globular domains (Fig. 1). The active site lies at the interface of two domains, C_A and C_B, which together constitute the catalytic core. A third, helical domain is connected to C_A by a linker (Switch C). In the structure of EF alone, the interface between the helical domain and the remainder of the protein buries 16 hydrophobic residues and 3600 $Å^2$ of surface area. None of these interactions are preserved in the EF-CaM complex, because CaM inserts itself between C_A and the helical domain. The EF-CaM interface buries 5900 $Å^2$ of solvent-accessible surface area between the two proteins so that the transition from EF to CaM/EF gains 2300 $Å^2$ of contact surface. In addition to the helical domain movement, Switches A, B, and C undergo large conformational changes in response to CaM binding (Fig. 1). Switches A and C are the predominant regions that interface with the helical domain in the EF-alone structure, and they also make substantial contact with CaM. Switch B is disordered in the structure of EF alone (Fig. 2). However, in the EF/CaM structure, Switch B becomes ordered and lies between Switch C and the nucleotide substrate (Fig. 2). Switch B consists of three amino acid residues — N583, E588, and D590 — that contribute significantly to catalysis; thus, juxtaposition of these residues to ATP accounts for over three orders of magnitude in CaM activation of EF.

Not only does EF share no structural similarity to mammalian adenylyl cyclase (mAC), but it also has a different catalytic mechanism from mAC. Residues from

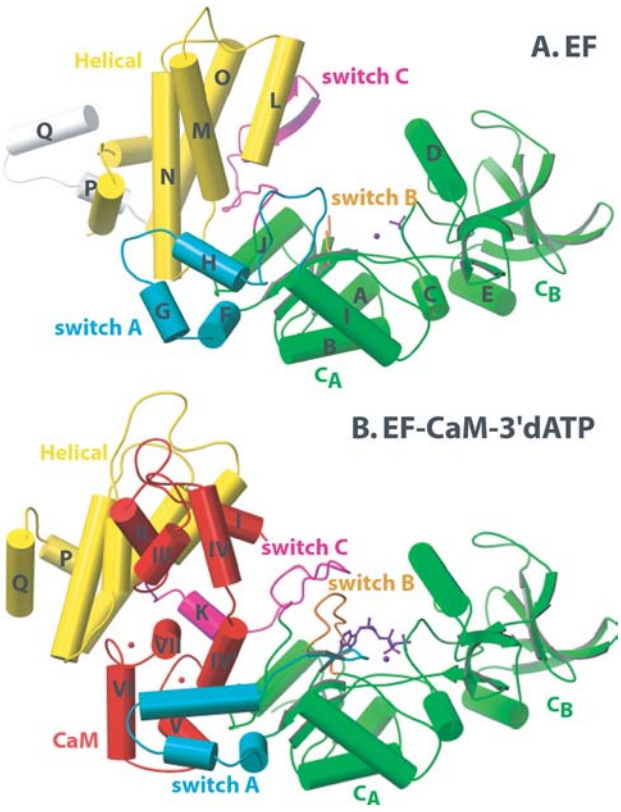

FIG. 1. Secondary structure representation of EF alone (A) and of EF-CaM-3'dATP complex (B). The CaM (red) is held on one side by a fingerlike projection of C_A (green) and on the other side by Switch C (magenta), and by the helical domain (yellow). Switch A and Switch B are cyan and orange, respectively. The 3'deoxy-ATP analog (purple) and metal (purple) are bound between the C_A and C_B domains (green), which form the active site.

six segments of EF form the substrate-binding pocket (Fig. 2). These residues form a network of hydrogen bonds and ionic interactions that completely encircle the triphosphate and ribose moieties, forming an enclosed cavity with openings at both ends. At the base of the cleft formed by domains C_A and C_B, a single metal interacts with the oxygens of the α and β phosphates of 3'-deoxy ATP. This metal is coordinated by two conserved aspartates, D491 and D493. H351 lies on the opposite side of the ribose from the metal and is well-positioned to interact with the reactive 3'OH when the ribose is in the 3'-*endo* conformation observed in the crystal (Fig. 2). This catalytic mechanism differs from that proposed for mAC, which is thought to utilize two-metal-ion catalysis [10].

The structure of the EF/CaM complex also provides new insight on how CaM binds to its effectors. The crystal structures of CaM — in complex with fragments

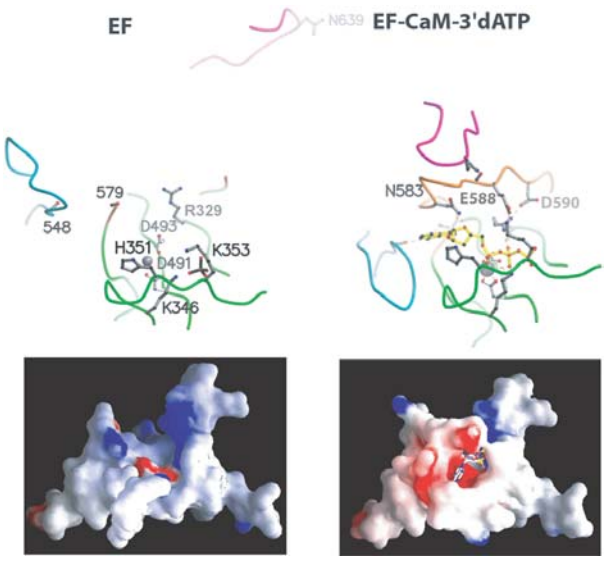

FIG. 2. Switch movement results in catalytic activation. Ball-and-stick (top) and surface (bottom) representations for the active EF alone catalytic site and the EF-CaM complex with 3'dATP. Top: C_A and Switches A, B, and C are green, blue, orange, and purple, respectively. 3'dATP in EF-CaM-3'dATP complex are yellow, while metal ions are gray. Bottom: Red and blue represent negative and positive surfaces, respectively.

from myosin light chain kinase (MLCK) [11], CaM kinase II α (CaMKIIα) [12], CaM kinase kinase (CaMKK) [13], and the Ca^{2+}-sensitive potassium channel [14] — define the canonical view of CaM/effector interaction, in which the hydrophobic faces of the two CaM lobes act as a clamp surrounding a target helix or helices (Fig. 3, B and C). The structure of the EF-CaM complex differs dramatically from this view. In the EF-CaM complex, the CaM lobes do not serve as a clamp, and four discrete regions from EF form a surface to contact CaM. The overall conformation of CaM is extended rather than compact, and the hydrophobic binding surface of the calcium-free N-terminus is buried within CaM rather than oriented toward the effector target. Only the interaction between the C-terminal lobe of CaM and EF helix H, which harbors 22% of the total CaM-binding surface, resembles the interaction observed with the recognition helix peptides from MLCK, and CAMKII (Fig. 3, D) [11, 12].

Acknowledgments

We are grateful to K. Moffat, W. Schildkamp, K. Brister, G. Navrotski, R. Pahl, Z. Ren, V. Srajer, T.-Y. Tang, and J. VonOsinski at APS BioCars 14-BM-C and 14-BM-D and A. Joachimiak and N. Duke at APS SBC 19-ID for their help in data collection. This work was supported by National Institutes of Health Grant Nos. GM53469, GM62548, and DA05778 to C. Drum. Use of the APS was supported by the U.S. Department of Energy, Office of Science, Office of Basic Energy Sciences, under Contract No. W-31-109-ENG-38. Figures are reprinted by permission from *Nature* [9], copyright 2002, Macmillan Publishers Ltd.

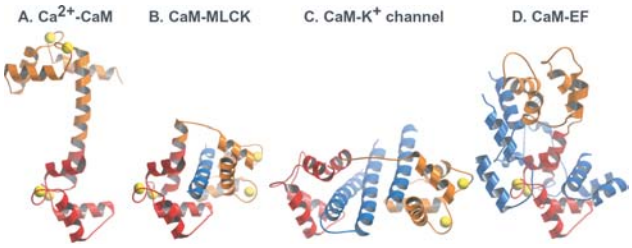

FIG. 3. Comparison of CaM conformations and of CaM/effector contacts. Ribbon representations of CaM alone (A), CaM in complex with the effector-derived peptides from MLCK (B), the Ca^{2+}-activated K^+ channel (C), and EF (D). The C-terminal domain (red) of CaM is aligned on the basis of helix VI of CaM. The CaM central helix and N-terminal domains are orange, and the effector peptides are blue.

References

[1] T. C. Dixon, M. Meselson, J. Guillemin, and P. C. Hanna, New England J. Medicine **341**(11), 815-826 (1999).
[2] C. Petosa, R. J. Collier, K. R. Klimpel, S. H. Leppla, and R. C. Liddington, Nature **385** (6619), 833-838 (1997).
[3] J. Mogridge, M. Mourez, R. J. Collier, J. A. Young, and K. A. Bradley, Nature **414** (6860), 225-229 (2001).
[4] A. Pannifer, T. Y. Wong, R. Schwarzenbacher et al., Nature **414**, 229-232 (2001).
[5] N. S. Duesbery, C. P. Webb, S. H. Leppla et al., Science **280**(5364), 734-737 (1998).
[6] W. J. Tang, J. Krupinski, and A. G. Gilman, J. Biol. Chem. **266**(13), 8595-8603 (1991).
[7] C. L. Drum, S. Z. Yan, R. Sarac, Y. Mabuchi, K. Beckingham, A. Bohm, Z. Grabarek, and W. J. Tang, J. Biol. Chem. **275**(46), 36334-36340 (2000).
[8] C. L. Drum, Y. Shen, P. A. Rice, A. Bohm, and W. J. Tang, Acta Crystallogr. D **57**, 1881-1884 (2001).
[9] C. L. Drum, S. Z. Yan, J. Bard, Y. Shen, D. Lu, S. Soelaiman, Z. Grabarek, A. Bohm, and W.-J. Tang, Nature **415**, 396-402 (2002).
[10] J. J. Tesmer, R. K. Sunahara, R. A. Johnson, G. Gosselin, A. G. Gilman, and S. R. Sprang, Science **285**(5428), 756-760 (1999).

[11] W. E. Meador, A. R. Means, and F. A. Quiocho, Science **257**(5074), 1251-1255 (1992).
[12] W. E. Meador, A. R. Means, and F. A. Quiocho, Science **262**(5140), 1718-1721 (1993).
[13] M. Osawa, H. Tokumitsu, M. B. Swindells, H. Kurihara, M. Orita, T. Shibanuma, T. Furuya, and M. Ikura, Nat. Struct. Biol. **6**(9), 819-824 (1999).
[14] M. A. Schumacher, A. F. Rivard, H. P. Bachinger, and J. P. Adelman, Nature **410**, 1120-1124 (2001).